# Sources of suspended sediments in salt marsh creeks

## Field measurements in China and the Netherlands

Sun, Jianwei; van Prooijen, Bram; Wang, Xianye; Hanssen, Jill; Xie, Weiming; Lin, Jianliang; Xu, Yuan; He, Qing; Wang, Zhengbing

**DOI**
10.1016/j.geomorph.2024.109206

**Publication date**
2024

**Document Version**
Final published version

**Published in**
Geomorphology

**Citation (APA)**
Sun, J., van Prooijen, B., Wang, X., Hanssen, J., Xie, W., Lin, J., Xu, Y., He, Q., & Wang, Z. (2024). Sources of suspended sediments in salt marsh creeks: Field measurements in China and the Netherlands. *Geomorphology*, *456*, Article 109206. https://doi.org/10.1016/j.geomorph.2024.109206

Geomorphology 456 (2024) 109206

Contents lists available at ScienceDirect

Geomorphology

journal homepage: www.journals.elsevier.com/geomorphology

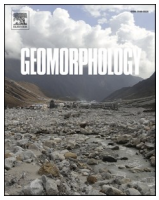

# Sources of suspended sediments in salt marsh creeks: Field measurements in China and the Netherlands

Jianwei Sun [a,b], Bram van Prooijen [b], Xianye Wang [a,*], Jill Hanssen [b,d], Weiming Xie [a], Jianliang Lin [c], Yuan Xu [a], Qing He [a], Zhengbing Wang [b,d]

[a] State Key Laboratory of Estuarine and Coastal Research, East China Normal University, 500 Dongchuan Road, Shanghai 200241, China
[b] Faculty of Civil Engineering and Geosciences, Delft University of Technology, Stevinweg 1, Delft 2628 CN, the Netherlands
[c] School of Marine Engineering and Technology, Sun Yat-sen University, Zhuhai 619082, China
[d] Deltares, P.O. Box 177, Delft 2628 CN, the Netherlands

ARTICLE INFO

*Keywords:*
Saltmarsh creeks
Sediment concentration
Sediment transport

ABSTRACT

Marsh creeks are perceived as important conduits for transporting water and sediment between mudflats and marshes. In order to advance the understanding of the transport mechanisms in creeks, the source and ultimate sink of sediment which moves between mudflats and marshes through creek channels need further investigation. Therefore, two field campaigns were conducted in two intertidal systems with varying sediment availability. The water depth, flow velocity, suspended sediment concentration, and bed level change were measured simultaneously in a marsh creek and on the adjacent mudflat in Chongming Island (China) and in Paulina Saltmarsh (the Netherlands). Paulina Saltmarsh is much smaller, more frequently flooded, and has lower sediment concentration than Chongming. These contrasting conditions allow for a comparison of transport mechanisms and functioning of the creek. Both systems first show that the high suspended sediment concentration (SSC) measured in marsh creeks is mainly the consequence of sediment advection rather than local erosion. In addition, erosion in marsh creeks is usually limited during ebb tides, reducing the export of sediment through these creeks. However, differences have been observed between two systems. The measured SSC was highly asymmetric between flood and ebb tides in Chongming. Large peaks in SSC during the flood period can be observed for most tidal cycles. The marsh creeks in Chongming therefore function as conduits for sediment import. Additionally, there are distinct overbank and underbank tides in Chongming. Sediment was trapped and retained in creeks during underbank tides, which can then be eroded and transported to the marsh during subsequent overbank tides. We also observed that mudflats in Chongming quickly recovered after erosion. These mechanisms have not been observed in Paulina Saltmarsh, where net sediment export via the marsh creek was observed due to a lack of abundant sediment in suspension during flood tides. Furthermore, the remaining bed surface of mudflats after an erosion event was stronger than before, limiting further erosion in Paulina Saltmarsh. These findings from the two systems indicate that the role of creeks in sediment import/export depends on the availability of sediment from mudflats, shedding light on nourishment strategies for salt marshes.

## 1. Introduction

Salt marshes are highly productive ecosystems that provide valuable functions, such as serving as habitats, acting as natural buffers against storms, and enhancing carbon sequestration (Benoit and Askins, 2002; Fagherazzi et al., 2012; Lockwood and Drakeford, 2021). These marsh systems are characterized by low relief. They expand vertically through accretion and horizontally via vegetation propagation. The capability of salt marshes to keep pace with accelerated sea level rise (SLR) largely depends on their accretion rates (Morris et al., 2002; Kirwan et al., 2010; Carrasco et al., 2021). This implies a need for sufficient sediment in the system outside the marsh, a transport mechanism to move sediment towards the marsh (i.e., sediment import), and conditions that ensure the sediment remains on the marsh.

The three-dimensional structure of salt marshes underscores the fact that their evolution is not only a result of internal factors but also closely

* Corresponding author.
*E-mail address:* xywang@sklec.ecnu.edu.cn (X. Wang).

https://doi.org/10.1016/j.geomorph.2024.109206
Received 20 October 2023; Received in revised form 10 April 2024; Accepted 11 April 2024
Available online 18 April 2024

linked with the co-evolution of adjacent mudflats. Mudflats are an important sediment reservoir for marshes, especially during storms when erosion in the former leads to deposition in the latter (Pannozzo et al., 2021; Hache et al., 2021). Sediment transported over the marsh edge is often trapped in the frontal area of marshes due to vegetation (Li and Yang, 2009; Lacy et al., 2020). Marsh creeks are the conduits connecting mudflats and salt marshes, serving as effective routes for sediment transport (Voulgaris and Meyers, 2004; Ganju et al., 2015; Ortals et al., 2021), and contributing to the growth of marsh surfaces, especially for the inner marshes. They deliver sediment onto the salt marsh during overbank tides, which leads to the accretion of salt marshes (Temmerman et al., 2005; Roner et al., 2016). Therefore, it is necessary to enhance our understanding of sediment transport regimes in salt marsh creeks.

Several field measurements have been carried out to unravel the complex hydrodynamics and sediment dynamics within the inter-tidal area (Carrasco et al., 2023; Ly and Huang, 2022). Particularly, dynamics of suspended sediment concentration (SSC) exhibit spatial and temporal variability, as erosion can be space and time dependent (Carniello et al., 2016). High SSC is occasionally observed in association with large tidal velocities. However, SSC does not always scale with local hydrodynamic forcings. High SSC values can also be found in association with relatively low tidal velocities (Green and Coco, 2007; Wang et al., 2012; Zhang et al., 2021). In such cases, the measured high sediment concentration may originate from erosion at other locations rather than from local erosion. To better understand the sediment transport regimes in marsh creeks, it is essential to determine the source of the measured suspended sediment concentration.

Erosion stands as an important factor which adds suspended sediment to the water column. It is a dynamic process shaped by the interplay of hydrodynamic forcings and the sediment bed characteristics (Winterwerp et al., 2018). While detailed erosion formulations, such as the Partheniades' erosion equation, offer insights into the quantifiable aspects of erosion. The parameters governing erosion, such as the critical shear stress, are often taken as constant and uniform values especially in numerical modes (van Leeuwen et al., 2010; Best et al., 2018; Wang et al., 2019). However, Sanford (2008), Mengual et al. (2016), Zhu et al. (2019) and Colosimo et al. (2020) had shown that the values of the critical shear stress are far from uniform across different spatial dimensions. The influence of such variations in critical shear stress, or in other words, availability of sediment, on the net sediment flux in creeks requires further investigation.

In this work, we analyzed the fieldwork data collected in two intertidal systems (Chongming Saltmarsh in China and Paulina Saltmarsh in the Netherlands). These two systems differ in suspended sediment concentration: the SSC in Chongming is substantially higher than in Paulina Saltmarsh. The data in Chongming was already partly presented in Xie et al. (2018). Here, we re-used the data for additional analysis and comparison with the Paulina dataset. This allows comparisons of different sediment transport regimes in marsh creeks across systems that differ in size, hydrodynamic conditions, and SSC levels, shedding light on the role of marsh creeks in delivering sediment under different conditions. In this work, we aim to (i) identify when the high SSC occurs in marsh creeks; (ii) interpret the source of this high SSC in the marsh creek; and (iii) compare sediment transport regimes within marsh creeks between two systems with very different sediment availability. With the comparison of sediment transport regimes between the two systems, the significance of sediment availability is highlighted. Our work enhances the understanding of the sediment sources and transport processes in marsh creeks, giving insights into management strategies that are essential for the resilience and development of salt marshes.

## 2. Materials and methods

### 2.1. Study area and field campaigns

Chongming is located in the Yangtze Estuary, China (Fig. 1a and b). The eastern part of Chongming Island consists of a wide salt marsh and multiple branched marsh creek systems. The salt marsh is approximately 18 $km^2$ and consists of many large creeks of 20–50 m in width and 0.1–3 m in depth (Jing et al., 2007; Ge et al., 2021). The slope of the marsh area is between 0.2 % and 0.5 %. According to the statistical data at Datong station, the annual runoff of the Yangtze River is $1.045 \times 10^{12}$ $m^3$ and the sediment flux was $1.52 \times 10^{11}$ kg in 2016 (CWRC, 2016). The annual averaged tidal range is approximately 2.6 m (Ding and Hu, 2020) and the extreme tidal range can reach up till 4.6 m. Because the Yangtze Estuary is very turbid, the sediment concentration in marsh creeks in Chongming can range between 0.1 g/L and 18 g/L (Wang et al., 2020). In addition, most precipitation and storm events occur in summer (June–September) in Chongming. Wave events during neap tides were captured in our measurements in Chongming.

Paulina Saltmarsh is located in the Western Scheldt Estuary, the Netherlands (Fig. 1c and d). Compared to the salt marsh in Chongming, Paulina Saltmarsh is much smaller with an area of approximately 0.6 $km^2$. It contains an old high marsh and a young low marsh. The marsh is dissected by a well-developed creek system of 0.3–7 m in width and 0.3–1.5 m in depth (Temmerman et al., 2005). The tidal range is 3.9 m on average, while spring tides can reach to 4.5 m (Oteman et al., 2019). Due to the relatively low-turbidity environment, the average SSC is around 0.05 g/L (Temmerman et al., 2003). Storm events generally occur in winter (November–March) in Paulina. There were no evident storm events in our measurements in Paulina.

To compare the two systems with different sediment availability, two summer field campaigns were conducted in Chongming from 2nd of August to 12th of August in 2016, and in Paulina Saltmarsh from 22nd of July to 31st of August in 2021.

In Chongming, two tripods with an ADV (Acoustic Doppler Velocimeter, Nortek AS, Norway), an ASM (Argus Surface Meter, ARGUS, Germany), and one RBR (Tide & Wave Loggers, RBR Limited, Canada) were deployed in a marsh creek (Fig. 1b #2) and on the adjacent mudflat (Fig. 1b #1), respectively. The ADV, ASM, and RBR at the creek site were 25, 25, and 7 cm above the bed, respectively; at the mudflat site, they were deployed 35, 35, and 5 cm above the bed, respectively. The SSC data obtained from the ASM were depth-averaged. Water depth, velocity, bed level change, and SSC were measured at these two sites.

In Paulina, we installed 2 frames with an ADV and an OBS-3+ (Optic Backscatter Sensor, Campbell Scientific, Australia) on the mudflat (Fig. 1d #1) and in the marsh creek (Fig. 1d #2) in Paulina Saltmarsh. We measured waves with a pressure sensor OSSI (the Ocean Sensor Systems Wave Gauge Blue, Wave Sensor Company, USA), which was deployed at the lower part of the mudflat (Fig. 1d #3). The ADV and the OBS at the mudflat were both deployed around 30 cm above the bed. At the marsh creek site, the ADV was also 30 cm above the creek bed, but due to the measurement failures for the OBS near the creek bed, we only acquired data from the OBS deployed 85 cm above the bed. We assume a fully mixed water column in this case. The OBS was synced with the ADV, and thus they measured for the same periods, bursts, and frequencies. More details of the setup for each instrument at all locations are shown in Table 1.

### 2.2. Data processing

The acoustic parameters (amplitude and correlation) of ADVs were used to remove erroneous data. Amplitudes larger than 100 and beam correlations higher than 70 were regarded as the valid velocity data (Zhu, 2017; Xie et al., 2018). To investigate sediment transport into and out of salt marsh systems, we focused on the along-creek component in the creek and cross-shore component of velocities on the mudflat. We

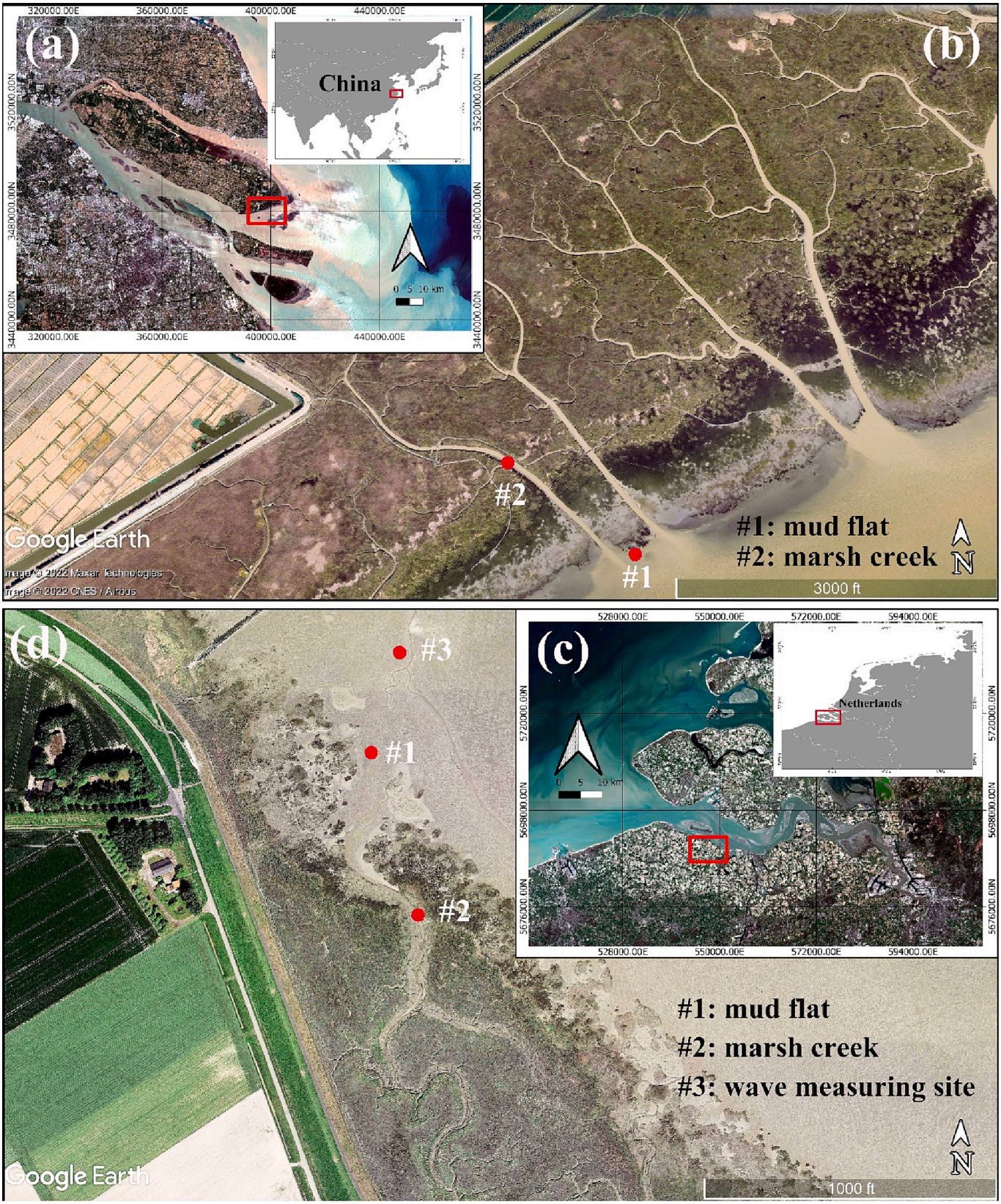


**Fig. 1.** (a) The Yangtze Estuary in China. Source aerial imagery: Landsat 9; (b) measuring sites in Chongming. Source aerial imagery: Google Earth; (c) the Westerschelde Estuary in the Netherlands. Source aerial imagery: Sentinel-2; (d) measuring sites in Paulina Saltmarsh. Source aerial imagery: Google Earth (Red circles indicate measuring locations).

**Table 1**
Set-up information of instruments in Chongming and Paulina Saltmarsh.

| Location | Instrument | Measuring intervals (s) | Length of burst (s) | Frequency (Hz) |
|---|---|---|---|---|
| Chongming | ADV | 600 | 60 | 64 |
| | ASM | 300 | 25 | 1 |
| | RBR | 300 | 128 | 4 |
| Paulina | ADV | 300 | 60 | 8 |
| Saltmarsh | OBS | 300 | 60 | 8 |
| | OSSI | 1 | 1 | 10 |

substituted the missing points by linear interpolation to get a more complete estimate for sediment flux.

OBS data were converted from the turbidity to sediment concentration, via calibration experiments using in-situ sediment samples. The calibration curves are shown in the supplementary material.

The cumulative single-point sediment flux per tidal inundation (*Fa*) was derived from the instantaneous data of velocity, water depth, and SSC (van Weerdenburg et al., 2021). The value of the integration for the entire tidal cycle indicates the import or export of sediment per tide. Positive values represent sediment import into the marsh while negative values represent sediment export out of the marsh.

$$F_a = \int_0^T (v \bullet h \bullet c)\, dt \tag{1}$$

where $v$ represents the velocity (m/s) in along-creek direction within the creek and in the cross-shore direction on the mudflat, $h$ is the water depth (m), $c$ is the suspended sediment concentration (g/L), and $T$ is the tidal period (s). As mudflats and creeks surfaces are drained of water with every tide, the tidal period is defined as the interval between two dry periods.

To better understand whether the erosion results from the current or waves, the shear stress induced by current and by waves were calculated separately (MacVean and Lacy, 2014). We used the same method as Zhu et al. (2016) and Xie et al. (2018) to obtain the bed shear stress. The wave shear stress was only considered on the mudflat. The bed shear stress induced by waves ($\tau_w$) is normally derived from the significant bottom orbital velocity $U_\delta$ and wave friction coefficient $f_w$:

$$\tau_w = \frac{1}{4}\rho_w f_w U_\delta^2 \tag{2}$$

where $\rho_w = 1025\ \mathrm{kg/m^3}$, which is the sea water density at the temperature of 21 °$C$ and the salinity of 35 ppt (Newton and Mudge, 2003). $A_\delta$ is the significant orbital excursion (m) and $U_\delta$ is the significant orbital velocity (m/s). They can be expressed as follows:

$$A_\delta = \frac{\mathrm{H}}{2sinh(kh)} \tag{3}$$

$$U_\delta = \omega A_\delta = \frac{\pi H}{Tsinh(kh)} \tag{4}$$

where $H$ is the wave height (m), $k$ is wave number defined as $k = 2\pi/L$ ($\mathrm{m^{-1}}$), $L$ is wave length defined as $L = (gT^2/2\pi)tanh(kh)$ (m), $h$ is the water depth (m), $T$ is wave period (s), and $\omega$ is angular velocity ($\mathrm{s^{-1}}$). The wave friction varies from hydraulic regime (Soulsby, 1983):

$$f_w = \begin{cases} 2Re_w^{-0.5}, Re_w \ll 10^5\ (laminar) \\ 0.0521Re_w^{-0.187}, Re_w \gg 10^5\ (smooth\ turbulent) \\ 0.237r^{-0.52}\ (rough\ turbulent) \end{cases} \tag{5}$$

where $Re_w$ is wave Reynolds number ($Re_w = \frac{U_\delta A_\delta}{\nu}$) and $r$ is relative roughness ($r = \frac{A_\delta}{k_s}$). $k_s$ is Nikuradse roughness related to the median grain size of bed sediment ($d_{50}$), and $\nu$ is the kinematic viscosity of water. We consider mudflats as a smooth bed. Therefore, we excluded the rough turbulent regime.

The shear stress induced by current ($\tau_c$) was considered both on mudflats and in marsh creeks. We used the logarithmic profile method for the current shear stress (Zhu et al., 2016), directly linking the bed shear stress to the mean flow. It is assumed that the current profile within boundary layers follows a logarithmic distribution.

$$\tau_c = \rho_w C_f \overline{U}^2 \tag{6}$$

where $C_f$ is the drag coefficient, which is taken a constant as 0.0025, and $\overline{U}$ is the burst-averaged velocities (m/s) obtained from the ADV.

## 3. Results

### 3.1. Chongming

In Chongming, the elevation of the marsh near the creek measuring site lies between mean high water neap (MHWN) and mean high water spring (MHWS), indicating that overbank tides and underbank tides occur. Overbank tides are tidal cycles when water can overtop the banks of a creek, whereas underbank tides refer to those when water levels are contained within the creek. Overbank flow only occurred during spring tides. Because of the diurnal inequality, one overbank tide and one successive underbank tide were observed (Fig. 2a, from T1 to T9). The water level did not exceed the bank level during neap tides, resulting in underbank tides (Fig. 2a, from T10 to T19). The velocities during the overbank tide, which reached approximately 0.8 m/s in the creek and 0.15 m/s on the mudflat, were higher compared to the velocities during the underbank tide, which were approximately 0.3 m/s in the creek and 0.05 m/s on the mudflat (Fig. 2b1 and b2). Larger ebb velocities were observed in the creek during overbank tides as more water from the marsh was concentrated into the creek, while larger flood velocities were observed during underbank tides due to the flood-dominant tidal asymmetry (Fig. 2b1).

A significant SSC peak of approximately 4 g/L was observed at the beginning of flood tides for most tidal cycles in the creek (Fig. 2c). This high flood SSC led to a slight accretion of the creek bed at the beginning of each overbank tide (Fig. 2d1). After the flood peak, the measured SSC in the creek decreased significantly and stayed at a relatively low value of <1 g/L. Local erosion of approximately 20 mm initially occurred in the creek (Fig. 2d1), leading to a slight increase in SSC to 0.9 g/L (Fig. 2c1). However, this increase in SSC was not as substantial as the flood peak of SSC at the beginning of the tidal cycle. During ebb tides, an additional 10 mm erosion occurred in the creek until the late stage of the ebb tide. After that, a deposition of approximately 7 mm occurred instead. Local erosion from the creek bed can contribute to an increased SSC during overbank tides. During the subsequent underbank tide, a high flood SSC of approximately 3 g/L was also observed, but the creek bed remained stable with no evident erosion or deposition (Fig. 2c1). Contrarily, the SSC on the mudflat did not always exhibit a large flood peak which was observed in the creek.

During the last few measuring days (T13–T19), a sudden rise of SSC was observed with low velocities at both locations (Fig. 2b and c). This increase in SSC was associated with the significant erosion of mudflats (Fig. 2d). Abundant sediment from the erosion of mudflats led to an increase in SSC at two locations. The SSC remained high during the entire tidal cycle. During the period from T13 to T19, a slight deposition occurred in the creek (Fig. 2d2).

### 3.2. Paulina

In Paulina Saltmarsh, overbank tides were observed during the entire measurement period (Fig. 3a), even during neap tidal cycles (e.g., from T20 to T24). This is because the measurements were conducted in the marsh creek at the young lower marsh. Higher velocities exceeding 0.3 m/s were observed in the marsh creek than on the mudflat (Fig. 3b). The

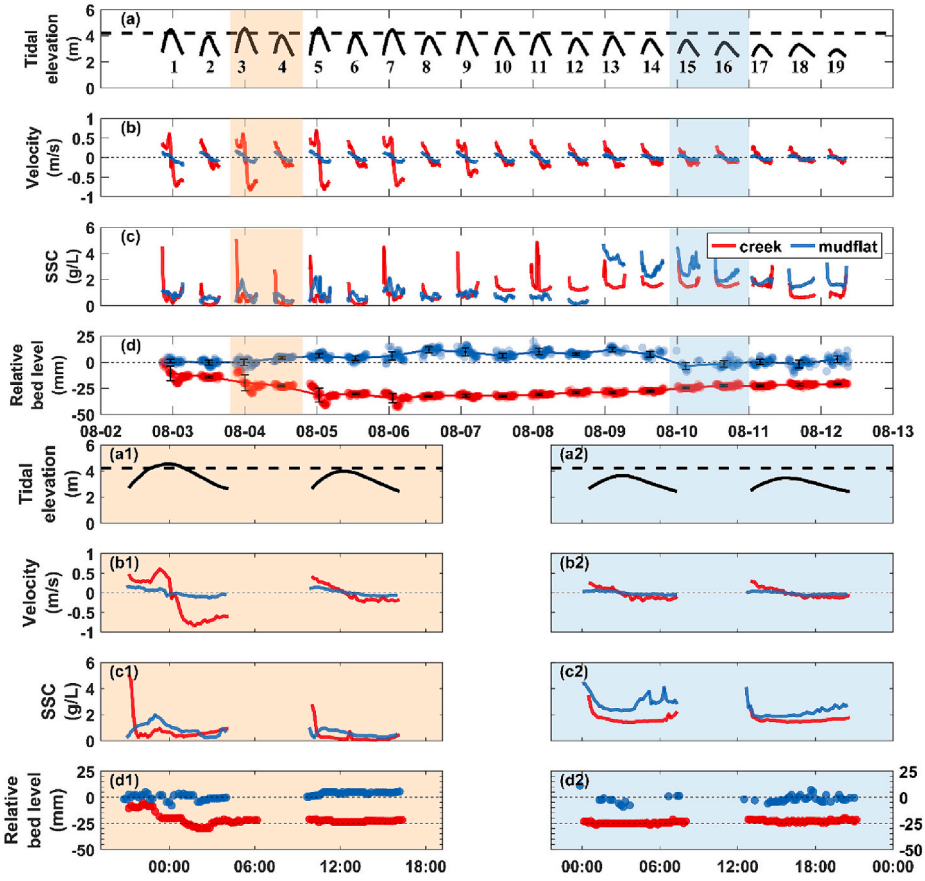


**Fig. 2.** Time series of (a) tidal elevation (the dashed line represents the elevation of the creek bank at the measuring location); (b) along-creek velocity in the creek and cross-shore velocity on the mudflat (flood velocity is positive); (c) the suspended sediment concentration observed by OBS-3A; (d) the relative bed level to the initial bed level of measurements in the marsh creek (red) and on the mudflat (blue) in Chongming. Negative values indicate erosion and positive values indicate deposition comparing with the initial bed level. The error bar indicates the standard deviation during each tidal cycle. Subfigures below (a1, a2, b1, b2, c1, c2, d1 and d2) are shown to provide more details during highlighted tidal cycles.

SSC in Paulina was notably lower compared to the SSC in Chongming. However, a relatively high SSC of 0.23 g/L occurred during the first two days of the measuring period (Fig. 3c, from T1 to T4). SSC peaks occurred during flood tides in the marsh creek, accompanied by evident erosion of mudflats, e.g., T3 and T4 (Fig. 3c1 and d1). For the remaining measurements, SSC in the marsh creek generally stayed relatively consistent, maintaining a low value of <0.08 g/L. However, the SSC on the mudflat occasionally fluctuated during some tidal cycles, for example, T13, T18 and T21. The measuring point of the mudflat bed remained relatively stable after the erosion during T4, while the creek bed showed considerable variation within tidal cycles (Fig. 3d2). In Paulina Saltmarsh, erosion of mudflats contributed to the sediment transport into the marsh creeks, leading to a notable increase in SSC within the marsh creek (e.g., T3 and T4). However, when the sediment supply from the mudflat decreased, the SSC in marsh creeks was affected by the erosion of the creek bed.

## 4. Discussion

### 4.1. Different sediment sources under varying dynamic regimes

In Chongming, the SSC in the creek showed specific patterns depending on tidal elevations. The average SSC during overbank tides (T1, T3, T5 and T7) was larger than during underbank tides (T2, T4, T6 and T8) (Fig. 4a). During overbank tides (during T1, T3, T5, T7), an evident current shear stress larger than 0.6 Pa was observed (Fig. 4b). At the same time, the creek experienced considerable erosion during each overbank tide (Fig. 2d). These indicate that tidal currents played an important role in the erosion of Chongming creeks during overbank tides. However, this erosion of the creek induced by current shear stress did not result in the flood peak of SSC. From Fig. 2c1 and d1, it is evident that at the beginning of the flood tide with the high SSC, no local erosion but deposition occurred. Later on, significant erosion of the creek was observed with a slight increase of SSC. These observations indicate that local erosion of creek beds did not lead to a substantial SSC peak during flood tides. Therefore, the high SSC is not likely from local erosion but from the advection of the sediment from mudflats or from the creek sections located between the marsh creek entrance and the measurement site.

Considering that the asymmetry in sediment concentration between flood and ebb is key for residual sediment fluxes (Ganju et al., 2015; Nowacki and Ganju, 2019; Sun et al., 2024), the flood peaks of SSC observed during calm weather result in a flood-dominant asymmetry in SSC. This consequently leads to an influx of sediment into marsh creeks (Fig. 4c, from T2 to T12). Therefore, the marsh creek in Chongming generally functions as a conduit for importing sediment during calm weather. During underbank tides, sediment was imported and deposited in the marsh creek system, and during the subsequent overbank tide, the sediment deposited during underbank tides was eroded and was further delivered into the tributaries and also the marsh. The sequence between underbank flow and overbank flow in Chongming leads to a dynamic sediment stock that is eventually delivered to the marsh.

During events when the wave shear stress on the mudflat was high (from T13 to T19), the average SSC increased both in the creek and on the mudflat. Erosion of mudflats and deposition in the creek have been observed during this period (Fig. 4c). These observations indicate that

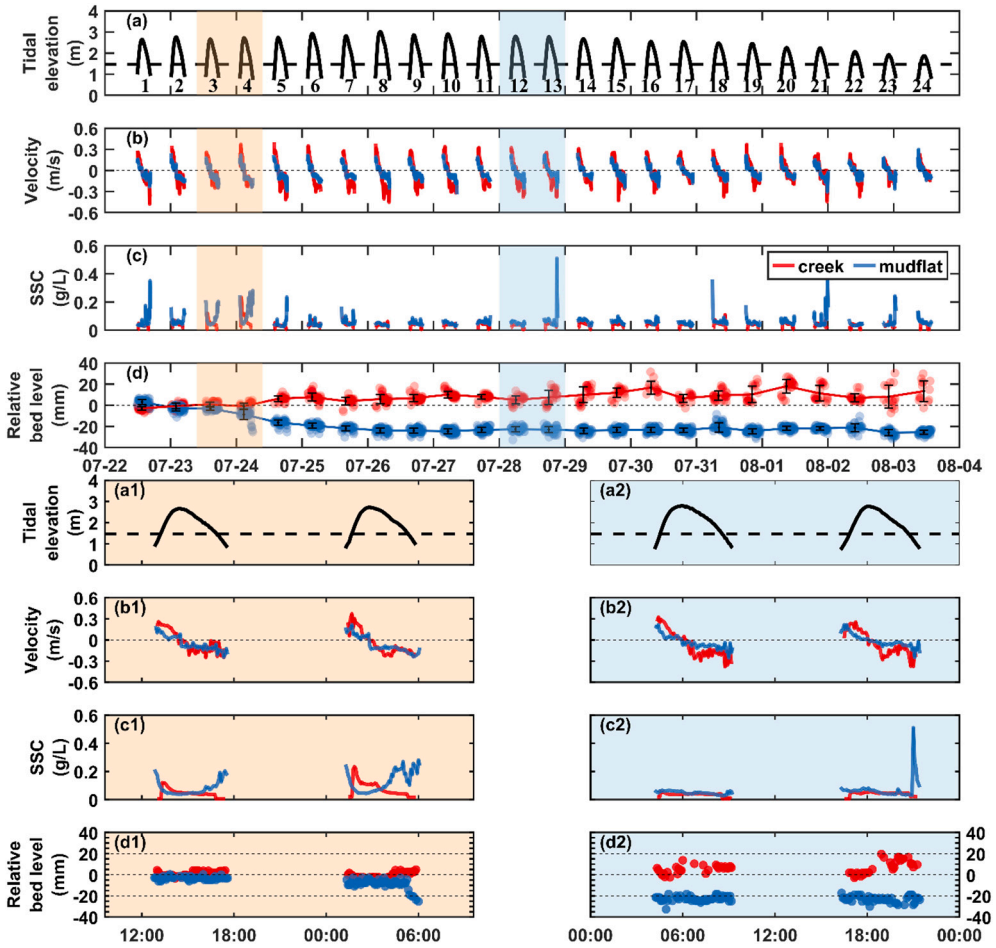


**Fig. 3.** Time series of (a) tidal elevation (the dashed line represents the elevation of the creek bank at the measuring location); (b) along-creek velocity in the creek and cross-shore velocity on the mudflat (flood velocity is positive); (c) the suspended sediment concentration observed by OBS-3A; (d) the relative bed level to the initial bed level of measurements in the marsh creek (red) and on the mudflat (blue) in Paulina Saltmarsh. Negative values indicate erosion and positive values indicate deposition comparing with the initial bed level. The error bar indicates the standard deviation during each tidal cycle. Subfigures below (a1, a2, b1, b2, c1, c2, d1 and d2) are shown to provide more details during highlighted tidal cycles.

waves re-suspended the sediment on the mudflat, leading to the high SSC at both locations. The current shear stress at both locations was low during neap tides (Fig. 4b). Therefore, waves played a more dominant role in SSC in the creek than tidal current during this period. Additionally, SSC remained high during entire tidal cycles (Fig. 2c, from T13 to T19), and sediment was still suspended even during slack water periods and also ebb tides. It is likely that the coarse sediment with higher settling velocities already deposited earlier (between the mud flat and the measurement location in the creek) with low velocities during neap tides, and fine sediment with lower settling velocities remained in the water column during wave events (Osborne and Greenwood, 1993), leading to a high SSC background value during tidal cycles. This high SSC throughout the tidal cycle resulted in more equal flood and ebb SSC values. Consequently, creeks tended to export sediment during wave events in Chongming (Fig. 4c). It is also important to note that, despite the high SSC in the creek induced by waves, significant deposition did not occur when the instruments were submerged during these tidal cycles (Fig. 2d2). Sediment settling and deposition mainly occurred during the shallow water periods (water depth $< 25$ cm) when the water level was below instrument sensors (Zhang et al., 2021). The hydrodynamics during these periods were too weak to suspend sediment, and hence we observed an increase in bed level of the creek during these periods (Fig. 4c).

The average SSC in Paulina Saltmarsh, measuring $<0.15$ kg/m$^3$, was notably lower than in Chongming (Fig. 5a). The SSC in the marsh creek did not show a clear correlation with the current shear stress in the marsh creek (Fig. 5a and b). However, during the T3 and T4 periods, relatively high SSC values were observed at both locations, coinciding with relatively large current and wave shear stresses on the mudflat (Fig. 5b). Furthermore, the mudflat experienced significant erosion during these tidal cycles (Fig. 5c), indicating that the high SSC was caused by the bed erosion of mudflats. The high SSC in the marsh creek in Paulina also responded more significantly to the erosion of mudflats rather than local erosion, which highlights the importance of the advection of sediment transport in the SSC in marsh creeks. The marsh creek played a role in importing sediment when mudflats experienced erosion. During other tidal cycles (from T6 to T24), the average SSC in the creek remained below 0.08 g/L. It seemed that the creek bed reached a dynamic equilibrium (Fig. 5c), where erosion in the creek only occurred with the presence of both erodible sediment layers and sufficient shear stress. These variabilities in sediment availability align well with the finding of Choi et al. (2023), where they found the newly deposited sediment exhibits high erodibility, and the critical shear stress for bed erosion decreases with the increase in bed elevation. In contrast with the case in Chongming, the absolute SSC levels in Paulina are limiting the amount of flux through the system. Consequently, the recovery ability of mudflats in Paulina is limited due to the insufficient sediment supply. Thus, no clear recovery of mudflats was observed after the erosion of approximately 20 mm. However, some SSC peaks on the mudflat occurred when the measuring point of the mudflat remained

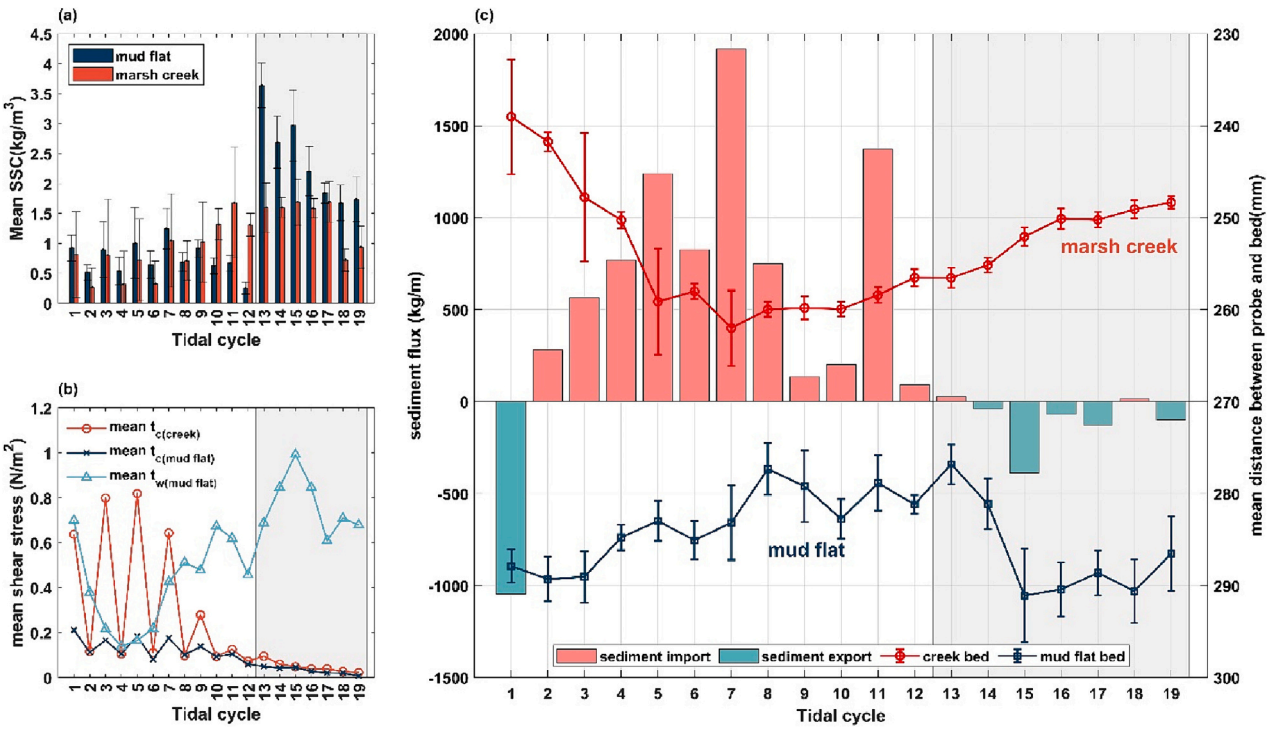


**Fig. 4.** (a) Tidal-averaged sediment concentration, (b) tidal-averaged shear stress induced by current and waves, and (c) residual sediment flux in the creek and bed level change of mudflats and creeks in Chongming (the error bar represents the standard deviation, and the shadow area indicates the special period when the high SSC occurred).

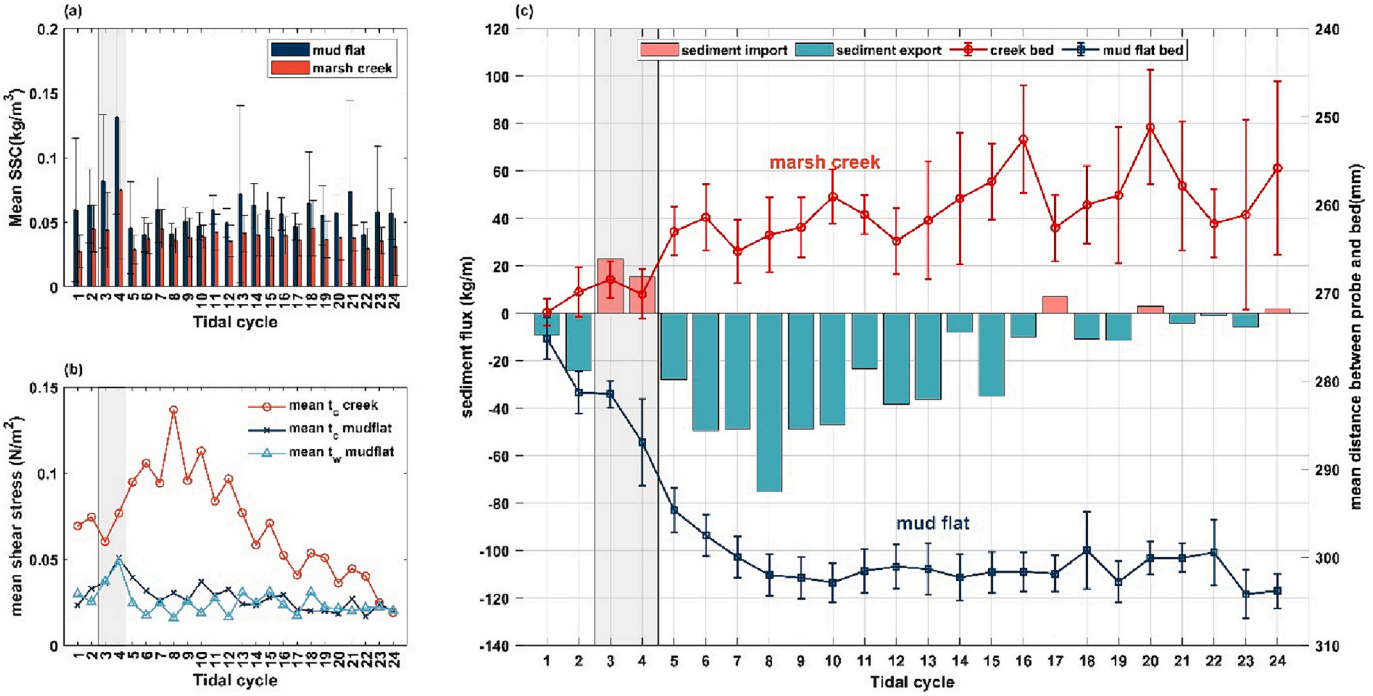


**Fig. 5.** (a) Tidal-averaged sediment concentration, (b) tidal-averaged shear stress induced by current and waves, and (c) residual sediment flux in the creek and bed level change of mudflats and creeks flux in Paulina Saltmarsh (the error bar represents the standard deviation, and the shadow area indicates the special period when the high SSC occurred).

relatively stable (e.g., T13, T18 and T21 in Fig. 3c). These peaks of SSC were likely originated from further offshore or erosion from other locations of mudflats.

During tidal cycles when sediment supply from mudflats was limited (e.g., from T5 to T19), the creek in Paulina Saltmarsh tended to export sediment (Fig. 5c). This is largely because the residual discharges in Paulina were generally negative due to the presence of overbank tides within the entire measurement period. This asymmetry in flow tended to export water and sediment. Furthermore, the sediment concentration differentials between flood and ebb tides in Paulina were relatively low

compared to those in Chongming. The absence of extremely high SSC during flood tides led to the consequence that the sediment concentration differential cannot counteract the exporting trend of the tidal current, resulting in sediment export. However, when erosion of mudflats occurred, leading to an increased sediment supply to the creek, sediment can be imported via the creek (e.g., T3 and T4). This highlights the importance of sediment availability of mudflats in determining the role of marsh creeks in sediment delivery.

It is necessary to note that our measurements only included wave events during neap tides in Chongming and excluded wave events in Paulina Saltmarsh. Seasonality of wave forcings may lead to different mechanisms for sediment transport (Callaghan et al., 2010). For example, in the low-turbidity environment, such as Paulina Saltmarsh, marsh creeks generally function as conduits for sediment export during the calm summer months, while the role of marsh creeks is likely to shift to importing sediment during the storm season in winter. This change is largely due to storm-induced wave events that erode mudflats, subsequently increasing the sediment available for transport towards the salt marsh during flood tides (Pannozzo et al., 2021). However, as observed during neap tides in Chongming, waves may also resuspend sediment and increase the SSC background during the entire tidal cycle. Further research regarding the wave impacts on sediment transport in marsh creeks is required.

Overall, both systems show that the SSC in marsh creeks is more responsive to the erosion of mudflats. Therefore, the high SSC is more likely the consequence of the advection rather than local erosion of the creek bed. The absolute SSC levels outside the intertidal system can influence the recovery of the mudflat after erosion, consequently affecting the sediment availability of mudflats and sediment fluxes in marsh creeks. These findings carry further implications for coastal protection, habitat conservation, and management practices. For example, human activities in coastal areas, such as dredging or land reclamation, can disrupt sediment dynamics. Therefore, understanding the interaction between mudflats and marsh creeks is essential for minimizing negative impacts on salt marsh ecosystems. In addition, recognizing mudflats as crucial sediment reservoirs for marsh creeks offers valuable insights for designing effective conservation and restoration strategies, which can enhance the resilience of salt marshes in the face of future sea-level rise.

### 4.2. Limited erosion in creeks

Current shear stress serves as an indicator of the erosive potential of tides. The critical shear stress is assumed to be the minimum shear stress

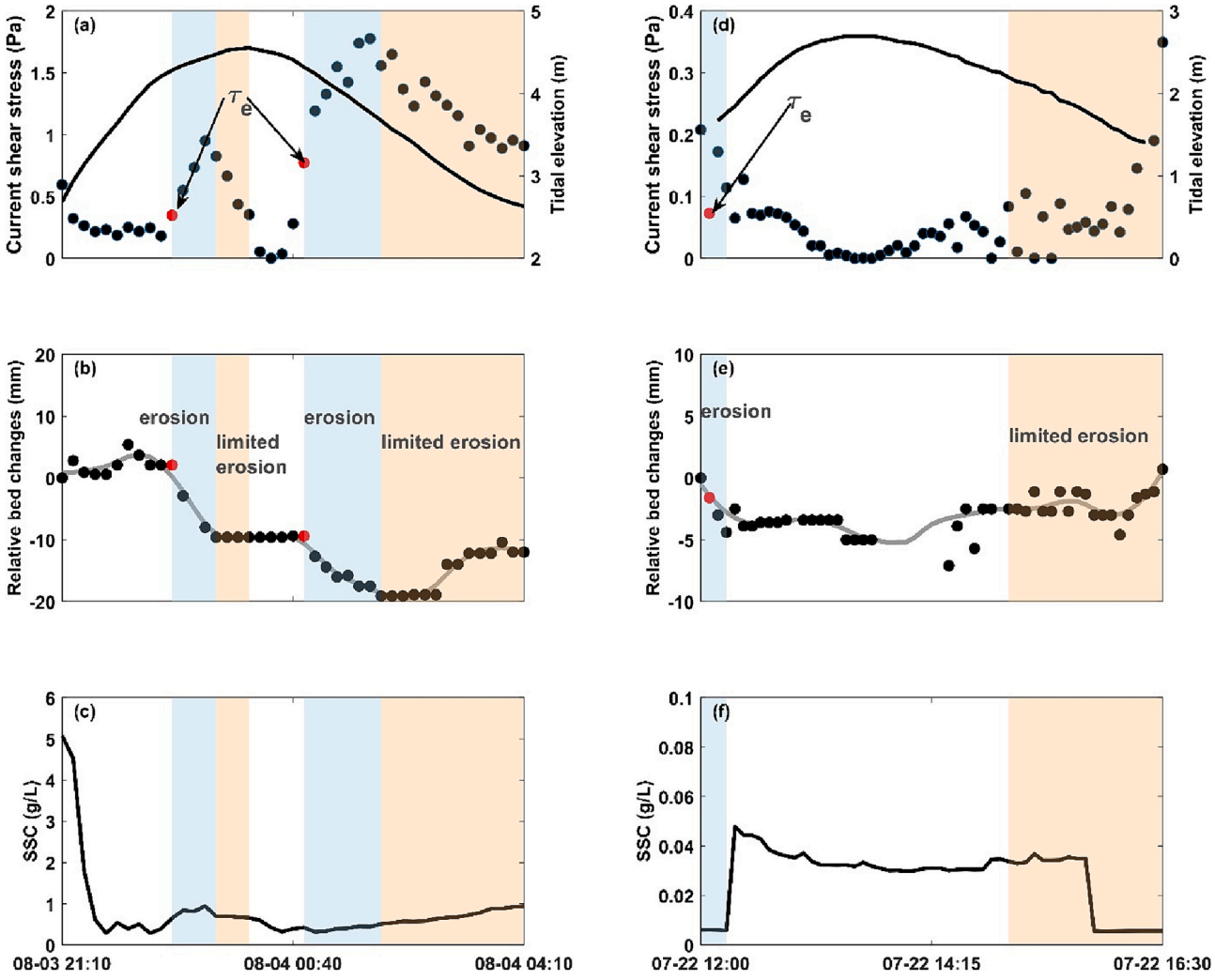


**Fig. 6.** Limited erosion in two systems. (a) Current shear stress (dotted line) and tidal elevations (solid line) in Chongming ($\tau_e$ represents the critical shear stress for erosion); (b) variations in bed level with respect to the initial bed level at the beginning of the tidal cycle in the creek in Chongming; (c) the measured SSC in Chongming; (d) current shear stress (dotted line) and tidal elevations (solid line) in Paulina Saltmarsh; (e) variations in bed level with respect to the initial bed level at the beginning of the tidal cycle in the creek in Paulina Saltmarsh; (f) the measured SSC in Paulina Saltmarsh. The erosion phases were highlighted in blue, and the limited erosion phases were highlighted in orange.

observed during the erosion phase in creeks (Fig. 6a and b). Together with bed level variations, it offers valuable insights into the interaction between tidal conditions and sediment bed dynamics during tidal cycles.

In Chongming, significant erosion occurred twice with different critical shear stresses for erosion. The first erosion event occurred during the late stage of the flood tide with a critical shear stress of 0.35 Pa and a bed level of 2.1 mm above the initial bed of the tidal cycle. After this erosion event, the bed level was 9.4 mm below the initial bed and remained stable until the subsequent erosion during the ebb tide. Yet, the second erosion event of a further 9.7 mm occurred during the early ebb tide and required a larger critical shear stress of 0.77 Pa. This increase in the critical shear stress could be related to consolidation, sediment properties, and benthic effects (Sanford, 2008; Brooks et al., 2021; Choi et al., 2023). After each erosion event, the erosion was then limited even with larger shear stresses, for example, current shear stresses ranging from 0.35 to 1 Pa during the flood tide and shear stresses ranging from 0.77 to 1.78 Pa during the ebb tide did not cause further erosion (Fig. 6a and b).

Both erosion events of the creek bed resulted in a slight rise in SSC (Fig. 6c), indicating that local bed erosion contributed to the SSC but was not the main sediment source for the initial flood peak of SSC, as only a slight increase of SSC was observed when local erosion occurred. Erosion of other locations, e.g., mudflats or the sections of the creek that lie between the marsh creek entrance and the measurement site, played an important role in flood SSC peaks.

In Paulina, erosion of 3.9 mm was observed during the beginning of the flood tide, with a potential critical shear stress of 0.07 Pa (Fig. 6d and e). This erosion led to a slight increase in SSC (Fig. 6f). The creek bed then remained relatively stable until the ebb tide. Subsequently, under shear stress ranging from 0.07 to 0.35 Pa during the ebb tide, deposition occurred instead of erosion, indicating that the creek bed after erosion exhibited less erodibility as the newly deposited sediment.

Because of the heterogeneity of sediment bed erodibility (Zhu et al., 2019; Colosimo et al., 2023), it is crucial to highlight that limited erosion occurs in creeks during tidal cycles. Erosion of a newly-formed fresh sediment bed and a deeper over-consolidated bed require different shear stresses. When considering erosion, especially in numerical models, a constant value of the critical shear stress is normally applied to determine erosion (Hu et al., 2015; Dastgheib et al., 2008; Zhou et al., 2022). However, the critical shear stress varies vertically in reality. Many factors contribute to this vertical variation of erodibility. In addition to the sediment properties (Sanford, 2008; Zhou et al., 2016), consolidation (Quaresma et al., 2004; Williams et al., 2008; Nguyen et al., 2020) and the formation of fluid mud (Maa et al., 1998; Neumeier et al., 2006) may play a role. Take Chongming as an example, a newly-formed bed from the previous underbank tide would be expected due to the moderate flow condition, and hence during the subsequent overbank tide, the erosion requiring a lower current shear stress occurred during the flood tide. During the ebb tide, larger shear stresses were observed due to the convergence of water to the creek, while the bed became more difficult to erode as the erosion progressed in depth. This sheds lights on the timing and conditions where the limited erosion can occur during tidal cycles. In addition, the critical shear stress was lower in Paulina than that in Chongming. We believe that the inundation duration may play an important role in this difference. The tidal regime is different between two systems, where an overbank tide and a successive underbank tide can be observed during spring tides in Chongming. The underbank tide would experience less inundation duration, allowing the sediment layers of marsh creeks to dry for a longer period. This, in turn, leads to a higher critical shear stress for the following overbank tide. On the other hand, there were consistently overbank tides in Paulina, potentially resulting in a lower critical shear stress compared to that in Chongming. Other factors, such as benthic activities (Harris et al., 2016), can also affect the critical shear stress. However, sediment grain size may not play a significant role in this case, as the grain sizes are similar in both systems (Yang et al., 2008; Willemsen et al., 2018).

Limited erosion was found during overbank ebb tides in both systems. This has impacts on the sediment flux in the creek. The limited erosion during ebb tides led to smaller ebb SSC, which indicated that the creek was unable to supply as much suspended sediment to the water column by erosion from waves/currents, as compared to what can be suspended from mudflats. This limited erosion in the creek reduces the amount of sediment transported out of the marsh system during ebb tides, which is beneficial for net sediment import.

## 5. Conclusion

The hydrodynamic and sediment dynamic regimes in marsh creeks vary between Chongming and Paulina Saltmarsh. In Chongming, overbank tides lead to significant erosion of the local creek bed, contributing to a small increase in SSC (<0.7 g/L). However, the flood peak of SSC during the beginning of tidal cycles, which can exceed 4.0 g/L, is not originated from local creek bed erosion but from the erosion of other areas, such as mudflats or the creek sections located between the marsh creek entrance and the measurement site. These high peaks of SSC cause the marsh creek to generally function as a conduit for sediment from the mudflat to be imported on to the marsh surface. In addition, sediment can be slightly deposited in marsh creeks during underbank tides, while it can be eroded during overbank tides in Chongming. The sequence between underbank flow and overbank flow in Chongming leads to a dynamic sediment stock that is eventually delivered to the marsh. Waves during neap tides increase the SSC levels, leading to more equal flood and ebb SSC during tidal cycles.

In Paulina Saltmarsh, overbank tides were observed during the entire measuring period, even during neap tides. In addition, the SSC is notably lower, generally below 0.08 g/L, compared to that in Chongming. Due to the absence of high flood SSC during calm conditions, the marsh creek generally serves as a conduit for sediment export. Only when erosion of mudflats occurred, the SSC in the marsh creek reached 0.23 g/L, and sediment was imported into the system via the creek. The creek bed was active in erosion and deposition among tidal cycles, while mudflats failed to recover after the erosion during our measurements, attributed to the low turbidity outside the intertidal system in Paulina.

By comparing two intertidal systems, sediment availability from mudflats, acting as the key factor for the role of marsh creeks in sediment transport, has been highlighted. In both systems, the SSC in marsh creeks slightly increases due to local erosion of the creek bed but responds more significantly to the erosion of mudflats, indicating that the sources of high suspended sediment in creeks result from the advection of sediment rather than local erosion of the creek bed. Additionally, the erodibility of creek beds varies vertically. Limited erosion of the creek bed occurred during ebb tides, reducing the export of sediment through marsh creeks. This work reveals sediment transport between mudflats and salt marshes through marsh creeks, emphasizing the significance of mudflats in marsh development and offering insights into sediment nourishment strategies for salt marshes.

## CRediT authorship contribution statement

**Jianwei Sun:** Writing – original draft, Methodology, Investigation, Formal analysis, Data curation. **Bram van Prooijen:** Writing – original draft, Supervision, Methodology, Conceptualization. **Xianye Wang:** Writing – review & editing, Supervision, Methodology, Data curation, Conceptualization. **Jill Hanssen:** Visualization, Investigation, Data curation. **Weiming Xie:** Visualization, Methodology, Investigation, Data curation. **Jianliang Lin:** Visualization, Validation. **Yuan Xu:** Visualization, Resources. **Qing He:** Supervision, Project administration. **Zhengbing Wang:** Supervision, Project administration.

## Declaration of competing interest

The authors declare that they have no known competing financial interests or personal relationships that could have appeared to influence the work reported in this paper.

## Data availability

Data will be made available on request.

## Acknowledgement

The support from Projects of Natural Science Foundation of China (NSFC) (U2040216, 42206169, 42276217, 51909101, U2243207), Shanghai Science and Technology Committee (Nos. 22dz1202700, 20DZ1204701, 21230750600), Shanghai Pujiang Program (22PJD020), Shanghai Sailing Program (23YF1410200), the project of Key Laboratory of Changjiang Regulation and Protection of Ministry of Water Resources (CX2023K05), Shandong Dongying City Cooperation Project (SXHZ-2022-02-10), and China Scholarship Council (CSC) are acknowledged. This study is conducted in the framework of the project "Coping with deltas in transition" within the Programme of Strategic Scientific Alliances between China and the Netherlands (PSA), financed by the Chinese Ministry of Science and Technology (MOST) and the Royal Netherlands Academy of Arts and Sciences (KNAW) (No. 2016YFE0133700).

This article has been partially grammar checked by ChatGPT, an OpenAI language model based in San Francisco, CA, USA.

## Appendix A. Supplementary data

Supplementary data to this article can be found online at https://doi.org/10.1016/j.geomorph.2024.109206.

## References

Benoit, L.K., Askins, R.A., 2002. Relationship between habitat area and the distribution of tidal marsh birds. Wilson Bull. 114, 314–323. https://doi.org/10.1676/0043-5643(2002)114[0314:RBHAAT]2.0.CO;2.

Best, Ü.S.N., Van der Wegen, M., Dijkstra, J., Willemsen, P.W.J.M., Borsje, B.W., Roelvink, D.J.A., 2018. Do salt marshes survive sea level rise? Modelling wave action, morphodynamics and vegetation dynamics. Environ. Model. Software 109, 152–166. https://doi.org/10.1016/j.envsoft.2018.08.004.

Brooks, H., Möller, I., Carr, S., Chirol, C., Christie, E., Evans, B., Spencer, K.L., Spencer, T., Royse, K., 2021. Resistance of salt marsh substrates to near-instantaneous hydrodynamic forcing. Earth Surf. Process. Landf. 46, 67–88. https://doi.org/10.1002/esp.4912.

Callaghan, D.P., Bouma, T.J., Klaassen, P., van der Wal, D., Stive, M.J.F., Herman, P.M.J., 2010. Hydrodynamic forcing on salt-marsh development: distinguishing the relative importance of waves and tidal flows. Estuar. Coast. Shelf Sci. 89, 73–88. https://doi.org/10.1016/j.ecss.2010.05.013.

Carniello, L., D'Alpaos, A., Botter, G., Rinaldo, A., 2016. Statistical characterization of spatiotemporal sediment dynamics in the Venice lagoon. J. Geophys. Res. Earth 121, 1049–1064. https://doi.org/10.1002/2015JF003793.

Carrasco, A.R., Kombiadou, K., Amado, M., Matias, A., 2021. Past and future marsh adaptation: lessons learned from the Ria Formosa lagoon. Sci. Total Environ. 790, 148082 https://doi.org/10.1016/j.scitotenv.2021.148082.

Carrasco, A.R., Kombiadou, K., Matias, A., 2023. Short-term sedimentation dynamics in mesotidal marshes. Sci. Rep. 13, 1921. https://doi.org/10.1038/s41598-022-26708-8.

Choi, S.M., Seo, J.Y., Ha, H.K., 2023. Contribution of local erosion enhanced by winds to sediment transport in intertidal flat. Mar. Geol. 465, 107171 https://doi.org/10.1016/j.margeo.2023.107171.

Colosimo, I., de Vet, P.L.M., van Maren, D.S., Reniers, A.J.H.M., Winterwerp, J.C., van Prooijen, B.C., 2020. The impact of wind on flow and sediment transport over intertidal flats. J. Mar. Sci. Eng. 8, 910. https://doi.org/10.3390/jmse8110910.

Colosimo, I., van Maren, D.S., de Vet, P.L.M., Winterwerp, J.C., van Prooijen, B.C., 2023. Winds of opportunity: the effects of wind on intertidal flat accretion. Geomorphology 439, 108840. https://doi.org/10.1016/j.geomorph.2023.108840.

CWRC (Changjiang Water Resource Committee), 2016. Bulletin of the Yangtze River Sediment. http://www/cjh/com.cn/.

Dastgheib, A., Roelvink, J.A., Wang, Z.B., 2008. Long-term process-based morphological modeling of the Marsdiep Tidal Basin. Mar. Geol. 256, 90–100. https://doi.org/10.1016/j.margeo.2008.10.003.

Ding, L., Hu, J., 2020. Influence of the salinity intrusion on island water source safety: a case study of the Chongming Island, China. In: Nguyen, K.D., Guillou, S., Gourbesville, P., Thiébot, J. (Eds.), Estuaries and Coastal Zones in Times of Global Change. Springer Water, Singapore, pp. 47–58. https://doi.org/10.1007/978-981-15-2081-5_4.

Fagherazzi, S., Kirwan, M.L., Mudd, S.M., Guntenspergen, G.R., Temmerman, S., D'Alpaos, A., van de Koppel, J., Rybczyk, J.M., Reyes, E., Craft, C., Clough, J., 2012. Numerical models of salt marsh evolution: ecological, geomorphic, and climatic factors. Rev. Geophys. 50 https://doi.org/10.1029/2011RG000359.

Ganju, N.K., Kirwan, M.L., Dickhudt, P.J., Guntenspergen, G.R., Cahoon, D.R., Kroeger, K.D., 2015. Sediment transport-based metrics of wetland stability. Geophys. Res. Lett. 42, 7992–8000. https://doi.org/10.1002/2015GL065980.

Ge, J., Yi, J., Zhang, J., Wang, X., Chen, C., Yuan, L., Tian, B., Ding, P., 2021. Impact of vegetation on lateral exchanges in a salt marsh-tidal creek system. J. Geophys. Res. Earth 126. https://doi.org/10.1029/2020JF005856 e2020JF005856.

Green, M.O., Coco, G., 2007. Sediment transport on an estuarine intertidal flat: measurements and conceptual model of waves, rainfall and exchanges with a tidal creek. Estuar. Coast. Shelf Sci. 72, 553–569. https://doi.org/10.1016/j.ecss.2006.11.006.

Hache, I., Karius, V., von Eynatten, H., 2021. Storm surge induced sediment accumulation on marsh islands in the southeastern North Sea: implications for coastal protection. Estuar. Coast. Shelf Sci. 263, 107629 https://doi.org/10.1016/j.ecss.2021.107629.

Harris, R.J., Pilditch, C.A., Greenfield, B.L., Moon, V., Kröncke, I., 2016. The influence of benthic macrofauna on the erodibility of intertidal sediments with varying mud content in three New Zealand estuaries. Estuar. Coasts 39, 815–828. https://doi.org/10.1007/s12237-015-0036-2.

Hu, Z., Wang, Z.B., Zitman, T.J., Stive, M.J.F., Bouma, T.J., 2015. Predicting long-term and short-term tidal flat morphodynamics using a dynamic equilibrium theory. J. Geophys. Res. Earth 120, 1803–1823. https://doi.org/10.1002/2015JF003486.

Jing, K., Ma, Z., Li, B., Li, J., Chen, J., 2007. Foraging strategies involved in habitat use of shorebirds at the intertidal area of Chongming Dongtan, China. Ecol. Res. 22, 559–570. https://doi.org/10.1007/s11284-006-0302-7.

Kirwan, M.L., Guntenspergen, G.R., D'Alpaos, A., Morris, J.T., Mudd, S.M., Temmerman, S., 2010. Limits on the adaptability of coastal marshes to rising sea level. Geophys. Res. Lett. 37 https://doi.org/10.1029/2010GL045489.

van Leeuwen, B., Augustijn, D.C.M., van Wesenbeeck, B.K., Hulscher, S.J.M.H., de Vries, M.B., 2010. Modeling the influence of a young mussel bed on fine sediment dynamics on an intertidal flat in the Wadden Sea. Ecol. Eng. 36, 145–153. https://doi.org/10.1016/j.ecoleng.2009.01.002.

Lacy, J.R., Foster-Martinez, M.R., Allen, R.M., Ferner, M.C., Callaway, J.C., 2020. Seasonal variation in sediment delivery across the bay-marsh interface of an estuarine salt marsh. J. Geophys. Res. Oceans 125, e2019JC015268. https://doi.org/10.1029/2019JC015268.

Li, H., Yang, S.L., 2009. Trapping effect of tidal marsh vegetation on suspended sediment, Yangtze Delta. J. Coast. Res. 25, 915–924. https://doi.org/10.2112/08-1010.1.

Lockwood, B., Drakeford, B.M., 2021. The value of carbon sequestration by saltmarsh in Chichester Harbour, United Kingdom. J. Environ. Econ. Policy 10, 278–292. https://doi.org/10.1080/21606544.2020.1868345.

Ly, T.N., Huang, Z.-C., 2022. Real-time and long-term monitoring of waves and suspended sediment concentrations over an intertidal algal reef. Environ. Monit. Assess. 194, 839. https://doi.org/10.1007/s10661-022-10491-0.

Maa, J.P.-Y., Sanford, L., Halka, J.P., 1998. Sediment resuspension characteristics in Baltimore Harbor, Maryland. Mar. Geol. 146, 137–145. https://doi.org/10.1016/S0025-3227(97)00120-5.

MacVean, L.J., Lacy, J.R., 2014. Interactions between waves, sediment, and turbulence on a shallow estuarine mudflat. J. Geophys. Res. Oceans 119, 1534–1553. https://doi.org/10.1002/2013JC009477.

Mengual, B., Cayocca, F., Le Hir, P., Draye, R., Laffargue, P., Vincent, B., Garlan, T., 2016. Influence of bottom trawling on sediment resuspension in the 'Grande-Vasière' area (Bay of Biscay, France). Ocean Dyn. 66, 1181–1207. https://doi.org/10.1007/s10236-016-0974-7.

Morris, J.T., Sundareshwar, P.V., Nietch, C.T., Kjerfve, B., Cahoon, D.R., 2002. Responses of coastal wetlands to rising sea level. Ecology 83, 2869–2877. https://doi.org/10.1890/0012-9658(2002)083[2869:ROCWTR]2.0.CO;2.

Neumeier, U., Lucas, C.H., Collins, M., 2006. Erodibility and erosion patterns of mudflat sediments investigated using an annular flume. Aquat. Ecol. 40, 543–554. https://doi.org/10.1007/s10452-004-0189-8.

Newton, A., Mudge, S.M., 2003. Temperature and salinity regimes in a shallow, mesotidal lagoon, the Ria Formosa, Portugal. Estuar. Coast. Shelf Sci. 57, 73–85. https://doi.org/10.1016/S0272-7714(02)00332-3.

Nguyen, H.M., Bryan, K.R., Pilditch, C.A., 2020. The effect of long-term aerial exposure on intertidal mudflat erodibility. Earth Surf. Process. Landf. 45, 3623–3638. https://doi.org/10.1002/esp.4990.

Nowacki, D.J., Ganju, N.K., 2019. Simple metrics predict salt-marsh sediment fluxes. Geophys. Res. Lett. 46, 12250–12257. https://doi.org/10.1029/2019GL083819.

Ortals, C., Cordero, O., Valle-Levinson, A., Angelini, C., 2021. Flows, transport, and effective drag in intertidal salt marsh creeks. J. Geophys. Res. Oceans 126. https://doi.org/10.1029/2021JC017357 e2021JC017357.

Osborne, P.D., Greenwood, B., 1993. Sediment suspension under waves and currents: time scales and vertical structure. Sedimentology 40, 599–622. https://doi.org/10.1111/j.1365-3091.1993.tb01352.x.

Oteman, B., Morris, E.P., Peralta, G., Bouma, T.J., van der Wal, D., 2019. Using remote sensing to identify drivers behind spatial patterns in the bio-physical properties of a saltmarsh pioneer. Remote Sens. (Basel) 11, 511. https://doi.org/10.3390/rs11050511.

Pannozzo, N., Leonardi, N., Carnacina, I., Smedley, R., 2021. Salt marsh resilience to sea-level rise and increased storm intensity. Geomorphology 389, 107825. https://doi.org/10.1016/j.geomorph.2021.107825.

Quaresma, V.S., Amos, C.L., Flindt, M., 2004. The influences of biological activity and consolidation time on laboratory cohesive beds. J. Sediment. Res. 74, 184–190. https://doi.org/10.1306/063003740184.

Roner, M., D'Alpaos, A., Ghinassi, M., Marani, M., Silvestri, S., Franceschinis, E., Realdon, N., 2016. Spatial variation of salt-marsh organic and inorganic deposition and organic carbon accumulation: inferences from the Venice lagoon, Italy. Adv. Water Resour. 93, 276–287. https://doi.org/10.1016/j.advwatres.2015.11.011.

Sanford, L.P., 2008. Modeling a dynamically varying mixed sediment bed with erosion, deposition, bioturbation, consolidation, and armoring. Comput. Geosci. 34, 1263–1283. https://doi.org/10.1016/j.cageo.2008.02.011.

Soulsby, R.L., 1983. Chapter 5. The bottom boundary layer of shelf seas. In: Johns, B. (Ed.), Physical Oceanography of Coastal and Shelf Seas, Elsevier Oceanography Series. Elsevier, pp. 189–266. https://doi.org/10.1016/S0422-9894(08)70503-8.

Sun, J., van Prooijen, B., Wang, X., Zhao, Z., He, Q., Wang, Z., 2024. Sediment fluxes within salt marsh tidal creek systems in the Yangtze Estuary. Geomorphology 449, 109031. https://doi.org/10.1016/j.geomorph.2023.109031.

Temmerman, S., Govers, G., Wartel, S., Meire, P., 2003. Spatial and temporal factors controlling short-term sedimentation in a salt and freshwater tidal marsh, Scheldt estuary, Belgium, SW Netherlands. Earth Surf. Process. Landf. 28, 739–755. https://doi.org/10.1002/esp.495.

Temmerman, S., Bouma, T.J., Govers, G., Wang, Z.B., De Vries, M.B., Herman, P.M.J., 2005. Impact of vegetation on flow routing and sedimentation patterns: three-dimensional modeling for a tidal marsh. J. Geophys. Res. Earth 110. https://doi.org/10.1029/2005JF000301.

Voulgaris, G., Meyers, S.T., 2004. Temporal variability of hydrodynamics, sediment concentration and sediment settling velocity in a tidal creek. Cont. Shelf Res. 24, 1659–1683. https://doi.org/10.1016/j.csr.2004.05.006.

Wang, X., Sun, J., Zhao, Z., 2020. Effects of river discharge and tidal meandering on morphological changes in a meso tidal creek. Estuar. Coast. Shelf Sci. 234, 106635 https://doi.org/10.1016/j.ecss.2020.106635.

Wang, Y., Wang, Y.P., Yu, Q., Du, Z., Wang, Z.B., Gao, S., 2019. Sand-mud tidal flat morphodynamics influenced by alongshore tidal currents. J. Geophys. Res. Oceans 124, 3818–3836. https://doi.org/10.1029/2018JC014550.

Wang, Y.P., Gao, S., Jia, J., Thompson, C.E.L., Gao, J., Yang, Y., 2012. Sediment transport over an accretional intertidal flat with influences of reclamation, Jiangsu coast, China. Mar. Geol. 291–294, 147–161. https://doi.org/10.1016/j.margeo.2011.01.004.

van Weerdenburg, R., Pearson, S., van Prooijen, B., Laan, S., Elias, E., Tonnon, P.K., Wang, Z.B., 2021. Field measurements and numerical modelling of wind-driven exchange flows in a tidal inlet system in the Dutch Wadden Sea. Ocean Coast. Manage. 215, 105941 https://doi.org/10.1016/j.ocecoaman.2021.105941.

Willemsen, P.W.J.M., Borsje, B.W., Hulscher, S.J.M.H., Van der Wal, D., Zhu, Z., Oteman, B., Evans, B., Möller, I., Bouma, T.J., 2018. Quantifying bed level change at the transition of tidal flat and salt marsh: can we understand the lateral location of the marsh edge? J. Geophys. Res. Earth 123, 2509–2524. https://doi.org/10.1029/2018JF004742.

Williams, J.J., Carling, P.A., Amos, C.L., Thompson, C., 2008. Field investigation of ridge–runnel dynamics on an intertidal mudflat. Estuar. Coast. Shelf Sci. 79, 213–229. https://doi.org/10.1016/j.ecss.2008.04.001.

Winterwerp, J.C., Zhou, Z., Battista, G., Van Kessel, T., Jagers, H.R.A., Van Maren, D.S., Van Der Wegen, M., 2018. Efficient consolidation model for morphodynamic simulations in low-SPM environments. J. Hydraul. Eng. 144, 04018055. https://doi.org/10.1061/(ASCE)HY.1943-7900.0001477.

Xie, W., He, Q., Wang, X., Guo, L., Zhang, K., 2018. Role of mudflat-creek sediment exchanges in intertidal sedimentary processes. J. Hydrol. 567, 351–360. https://doi.org/10.1016/j.jhydrol.2018.10.027.

Yang, S.L., Li, H., Ysebaert, T., Bouma, T.J., Zhang, W.X., Wang, Y.Y., Li, P., Li, M., Ding, P.X., 2008. Spatial and temporal variations in sediment grain size in tidal wetlands, Yangtze Delta: on the role of physical and biotic controls. Estuar. Coast. Shelf Sci. 77, 657–671. https://doi.org/10.1016/j.ecss.2007.10.024.

Zhang, Q., Gong, Z., Zhang, C., Lacy, J., Jaffe, B., Xu, B., Chen, X., 2021. The role of surges during periods of very shallow water on sediment transport over tidal flats. Front. Mar. Sci. 8 https://doi.org/10.3389/fmars.2021.599799.

Zhou, Z., van der Wegen, M., Jagers, B., Coco, G., 2016. Modelling the role of self-weight consolidation on the morphodynamics of accretional mudflats. Environ. Model. Software 76, 167–181. https://doi.org/10.1016/j.envsoft.2015.11.002.

Zhou, Z., Wu, Y., Fan, D., Wu, G., Luo, F., Yao, P., Gong, Z., Coco, G., 2022. Sediment sorting and bedding dynamics of tidal flat wetlands: modeling the signature of storms. J. Hydrol. 610, 127913 https://doi.org/10.1016/j.jhydrol.2022.127913.

Zhu, Q., 2017. Sediment Dynamics on Intertidal Mudflats: A Study Based on In Situ Measurements and Numerical Modelling.

Zhu, Q., van Prooijen, B.C., Wang, Z.B., Ma, Y.X., Yang, S.L., 2016. Bed shear stress estimation on an open intertidal flat using in situ measurements. Estuar. Coast. Shelf Sci. 182, 190–201. https://doi.org/10.1016/j.ecss.2016.08.028.

Zhu, Q., van Prooijen, B.C., Maan, D.C., Wang, Z.B., Yao, P., Daggers, T., Yang, S.L., 2019. The heterogeneity of mudflat erodibility. Geomorphology 345, 106834. https://doi.org/10.1016/j.geomorph.2019.106834.